Quantum Monte Carlo study of static properties of one ^{3}He atom in superfluid ^{4}He

J. Boronat and J. Casulleras
Departament de Física i Enginyeria Nuclear, Campus Nord B4-B5, Universitat Politècnica de Catalunya, E-08034 Barcelona, Spain
(Received 17 July 1998)

The local environment and the energetic properties of one ^{3}He atom solved in bulk superfluid ^{4}He are studied by means of the diffusion Monte Carlo method. The chemical potential of the ^{3}He impurity is calculated with a generalized reweighting method which allows for a reliable estimation of this quantity. Results for the chemical potential, radial distribution and structure functions, volume-excess parameter, and effective mass are given for several pressures and compared with available experimental data. An overall agreement with experiment is obtained except for the kinetic energy of the ^{3}He atom which, in accordance with previous theoretical estimations, appears to be considerably larger than determinations from deep-inelastic neutron scattering. [S0163-1829(99)11713-2]

I. INTRODUCTION

Isotopic ^{3}He-^{4}He mixtures have deserved theoretical and experimental interest for many years due to their unique properties.[1,2] Among them one may recognize the only isotopic mixture which remains stable at a certain ^{3}He concentration down to zero temperature, and the only liquid system in which the two quantum statistics, bosons (^{4}He) and fermions (^{3}He), are put together and one influences the other through the interatomic potential. As a result of this interplay, it has been observed both experimentally and theoretically, that the ^{4}He superfluid fraction decreases and simultaneously the ^{4}He condensate fraction increases when the ^{3}He concentration increases. On the other hand, the ^{3}He momentum distribution in the mixture appears largely influenced by the presence of ^{4}He showing a considerably larger depletion above the Fermi momentum in comparison with pure ^{3}He. Experimental information on the ^{4}He condensate fraction (n_0) and the kinetic energy of both ^{4}He and ^{3}He in the mixture have been recently extracted from deep-inelastic neutron scattering.[3,4] These analysis show a large enhancement of n_0 with respect to pure ^{4}He, and ^{3}He kinetic energies very similar to the ones of pure ^{3}He. In contrast, all the theoretical calculations[5,6] have shown only a small increment of n_0 when the ^{3}He concentration (x) increases (mainly due to the change in the total density at a fixed pressure) and a ^{3}He kinetic energy appreciably larger.

The maximum solubility of ^{3}He in ^{4}He is $x^m = 0.066$ at zero pressure and presents a maxim value of $x^m = 0.095$ at $P \simeq 10$ atm. These x values are sufficiently small to stimulate the theoretical interest in describing microscopically the limit of zero ^{3}He concentration which, on the other hand, has also been experimentally analyzed and a number of characteristic properties are nowadays available.[2] From a theoretical viewpoint, this limiting system has been studied considering a single ^{3}He atom solved in bulk ^{4}He. The most useful approach in the past has been the variational method combined with the resolution of the hypernetted chain equations coupled[7,8] or not[9] to an Euler-Lagrange optimization procedure. The results obtained with this approach reproduce the energetic and structural properties of the system with a good accuracy but the impurity effective mass appears slightly underestimated.[10] The application of Monte Carlo methods, both variational[11] and *ab initio*,[12] to the impurity system in order to calculate a basic property as the chemical potential of the impurity in the bulk (μ_I), has been seriously hindered by the fact that μ_I results from the difference of two energy terms of order N, N being the number of particles. In fact, a straightforward application of the Monte Carlo method cannot estimate μ_I because the statistical fluctuations would mask it completely.

In the present calculation, the reported results for μ_I have been obtained using a particular reweighting procedure suitable for the diffusion Monte Carlo (DMC) method, which has allowed a direct calculation of μ_I with a statistical error reduced to a manageable level. Using this method, we have been able to obtain reliable results for μ_I that fit accurately the experimental data from the equilibrium up to the freezing ^{4}He densities. The local environment of the impurity, reflected in the crossed radial distribution and structure functions, has been studied by means of a pure estimator[13] to remove the bias associated to the trial wave function. We have, finally, focused our attention on the calculation of the impurity effective mass and its kinetic energy for several densities. As in previous quantum Monte Carlo (QMC) applications,[5,12] the effective mass is extracted from the diffusion coefficient in imaginary time and, in spite of some uncertainties inherent to the extrapolated estimator used in this calculation, a reasonable agreement with recent experimental determinations[14,15] is attained. Our results concerning the kinetic energy of the impurity, derived from the Hellmann-Feynman theorem, avoid the residual importance-sampling dependence and show values which are definitely larger than the experimental data, as pointed out previously in variational[6,9] and path integral Monte Carlo (PIMC)[12] calculations.

The outline of the paper is as follows. In the next section we briefly introduce the DMC algorithm for the impurity system and present a DMC reweighting technique that permits a direct estimation of arbitrarily small differences. In Sec. III, we present the results and compare them with available experimental and theoretical data. We close in Sec. IV with the summary and final remarks.

II. THE DIFFUSION MONTE CARLO METHOD WITH REWEIGHTED CONFIGURATIONS

The DMC method[16–18] allows for a very accurate description of the ground-state properties of an interacting N-body system. In the DMC formulation the imaginary-time Schrödinger equation for the function $f(\mathbf{R},t)=\Psi_T(\mathbf{R})\Phi(\mathbf{R},t)$,

$$-\frac{\partial f(\mathbf{R},t)}{\partial t}=\sum_{i=1}^{N}-D_i[\nabla_i^2 f(\mathbf{R},t)-\nabla_i\cdot(\mathbf{F}_i(\mathbf{R})f(\mathbf{R},t))]+(E_L(\mathbf{R})-E)f(\mathbf{R},t), \quad (1)$$

is turned into a stochastic process which provides a sample of configuration points $\mathbf{R}$ (walkers) and weights $w(\mathbf{R})$ in a $3N$-dimensional space, whose probability distribution is given by $f(\mathbf{R},t)$.$\Psi_T(\mathbf{R})$ is a time-independent trial wave function that acts as an importance-sampling function, and $\Phi(\mathbf{R},t)$ is the exact wave function of the system. In this form, the Schrödinger equation appears as a diffusionlike differential equation with a diffusion, drift, and branching terms corresponding to the first, second, and third terms of the right-hand side of Eq. (1), respectively. In Eq. (1), $E_L(\mathbf{R})=\Psi_T(\mathbf{R})^{-1}H\Psi_T(\mathbf{R})$ is the local energy, $\mathbf{F}_i(\mathbf{R})=2\Psi_T(\mathbf{R})^{-1}\nabla_i\Psi_T(\mathbf{R})$ is the quantum drift force, and $D_i=\hbar^2/(2m_i)$ acts as the free-diffusion constant of the i particle. At sufficiently long imaginary times the probability density evolves to a stationary solution given by $\Phi_0(\mathbf{R})\Psi_T(\mathbf{R}),\Phi_0(\mathbf{R})$ being the ground-state wave function from which the exact ground-state energy is obtained as the average of the local energy $E_L(\mathbf{R})$.

Let us now turn to the implementation of the reweighting method. In the DMC algorithm, the distribution probability of the walkers is modified in every single operation. Consider in particular the stochastic process originated by the diffusion term, which is a random Gaussian displacement $\mathbf{R}\rightarrow\mathbf{R}'$. The new weight and distribution probability are $w'(\mathbf{R}')=w(\mathbf{R})$ and $p'(\mathbf{R}')=\int e^{-[(\mathbf{R}'-\mathbf{R})^2/4D\Delta t]}p(\mathbf{R})\,d\mathbf{R}$, respectively. In this stochastic process we can make use again of importance sampling in order to perform a modified diffusion random displacement. In this case, if the transition probability of going from $\mathbf{R}$ to $\mathbf{R}'$ following the modified diffusion process is $G(\mathbf{R}'-\mathbf{R})$, the new distribution probability is given by

$$p'(\mathbf{R}')=\int G(\mathbf{R}'-\mathbf{R})p(\mathbf{R})\,d\mathbf{R}, \quad (2)$$

and the statistical sample of walkers provides unchanged averaged values if one uses accordingly a new weight given by

$$\frac{w'(\mathbf{R}')}{w(\mathbf{R})}=\frac{e^{-[(\mathbf{R}'-\mathbf{R})^2/4D\Delta t]}}{G(\mathbf{R}'-\mathbf{R})}. \quad (3)$$

This means that a system can be studied using a variety of diffusion random laws, although the efficiency of the method will be related to the magnitude of the changes. In general, the modification has to be small enough so that the same configuration space is sampled.

The reweighting method is especially useful in the calculation of differences between two almost identical systems. Performing independent samplings for both systems generates a global uncorrelated noise that prevents a direct measure of the difference. However, this problem can be avoided considering that given a common starting configuration point $\mathbf{R}$, a single deterministic drift process brings both walkers to new positions $\mathbf{R}_1(\mathbf{R})$ and $\mathbf{R}_2(\mathbf{R})$ which are very close (in particular, separated a distance much smaller than the typical size of a random Gaussian displacement). The configuration region attainable after the subsequent diffusion process is the same, and the transition probabilities to a final point $\mathbf{R}'$ are almost equal. Equations (2) and (3) may then be used to change both probabilities $\exp[-(\mathbf{R}'-\mathbf{R}_i)^2/(4D\Delta t)]$ into a common one $G_1(\mathbf{R}'-\mathbf{R}_1)\equiv G_2(\mathbf{R}'-\mathbf{R}_2)$. The key point is, therefore, that there is no need of taking averages using two independent walkers for the two systems, and it may be highly preferable to use *correlated walkers*, in the sense of carrying a single random walk to obtain statistical values for both systems. Furthermore, notice that this technique may be applied to modify the diffusion process of the whole walker, i.e., all the particles of the system, or only a subset of it.

The generalized reweighting method is an appropriate tool for studying the quantum liquid in which we are now interested. It is composed by $N-1$ ^{4}He particles and one ^{3}He atom (I) enclosed in a simulation box with periodic boundary conditions. The Hamiltonian of the system is

$$H=-D_4\sum_{i=1}^{N-1}\nabla_i^2-D_I\nabla_I^2+\sum_{i<j}^{N}V(r_{ij}), \quad (4)$$

and the trial wave function $\Psi_T(\mathbf{R})$ has been chosen to be of the Jastrow type

$$\Psi_T(\mathbf{R})=\exp\left(\sum_{i<j}^{N}u(r_{ij})\right) \quad (5)$$

without distinguishing between the (4,I) and (4,4) pairs of particles. This simplification in the wave function, known as average correlation approximation (ACA), has been used in several variational calculations[8,9] obtaining a quite good description of the impurity properties. In the DMC method the trial wave function acts only as a guiding wave function for the walkers driving them to regions where $\Phi_0(\mathbf{R})$ is expected to be large and thus a particular choice, as the ACA one in the present case, does not bias the expected value for the ground-state energy. On the other hand, the *sign* problem that would emerge in a simulation of a finite ^{3}He concentration in ^{4}He does not appear here and an exact energy for the system, apart from statistical uncertainties, can be safely obtained.

From the energetic viewpoint, the more fundamental quantity in the study of the ^{3}He impurity in ^{4}He is the impurity chemical potential or binding energy

$$\mu_I=\langle H(N+I)\rangle_{N+I}-\langle H(N)\rangle_N, \quad (6)$$

both energy estimations being evaluated at fixed volume $\Omega=N/\rho$. If the total number of particles is also conserved, and therefore one ^{4}He atom is substituted by the ^{3}He impurity, μ_I is given by

$$\mu_I=\mu_4+(\langle H[(N-1)+I]\rangle_{(N-1)+I}-\langle H(N)\rangle_N). \quad (7)$$

We have chosen the second option in which the difference between the two energy estimations is much less density

dependent than in Eq. (6), and moreover because it is more convenient if a correlated estimation of the difference is intended. The pure ^{4}He chemical potential μ_4 entering in Eq. (7) has been determined in a previous work using also the DMC method with a good agreement with experimental data.[19,20]

The drawback of an *ab initio* MC estimation of μ_I, that has precluded such a calculation for years, is that an independent calculation of $\langle H[(N-1)+I]\rangle_{(N-1)+I}$ and $\langle H(N)\rangle_N$ followed by its difference, produces a result completely hidden by the statistical error. In order to overcome this serious problem, we have directly sampled the difference by means of the reweighting method above introduced. Our purpose was to perform two *correlated* DMC runs, one of bulk ^{4}He and the other with one ^{3}He impurity. Equation (2) has allowed us to use the same environment for both the ^{3}He atom in the impurity system and the equivalent ^{4}He atom in the pure liquid. In fact, the drift of the surrounding $N-1$ particles in Eq. (1) is almost insensitive to the mass of the impurity, i.e., the resulting positions in the impurity system ($\mathbf{R}^I_{N-1}$) and in the pure phase ($\mathbf{R}^4_{N-1}$) are very close. One can decide then to change the diffusion process of the environment in the pure system in such a way that the transition probability $G(\mathbf{R}'_{N-1}-\mathbf{R}^4_{N-1})$ exactly matches that of the environment of the ^{3}He impurity, i.e.,

$$G(\mathbf{R}'_{N-1}-\mathbf{R}^4_{N-1}) \equiv \exp\left(-\frac{(\mathbf{R}'_{N-1}-\mathbf{R}^I_{N-1})^2}{4D_4\Delta t}\right). \tag{8}$$

This results in a modification of the weight of the pure system given by

$$\frac{w'(\mathbf{R}')}{w(\mathbf{R})} = \exp\Big[-\frac{1}{4D_4\Delta t}[(\mathbf{R}'_{N-1}-\mathbf{R}^4_{N-1})^2 - (\mathbf{R}'_{N-1}-\mathbf{R}^I_{N-1})^2]\Big]. \tag{9}$$

In this form, the statistical fluctuations coming from regions far from the impurity and its corresponding ^{4}He atom cancel exactly, and the remaining signal corresponds only to their local environment making feasible a direct estimation of μ_I.

In addition to the impurity chemical potential μ_I, the knowledge of other properties as the crossed radial distribution function $g^{(4,I)}(r)$, the impurity effective mass and its kinetic energy are also relevant in a microscopic characterization of the ^{3}He impurity. Expectation values of operators $\mathcal{O}$ that do not commute with the Hamiltonian H are, however, biased because the probability density is $\Psi_T(\mathbf{R})\Phi_0(\mathbf{R})$ and not $|\Phi_0(\mathbf{R})|^2$. Thus, the natural expectation values, called mixed estimators (m), have to be corrected in order to reduce or eliminate this systematic source of error. In the extrapolation methods,[21] this correction is approximated by

$$\langle\mathcal{O}\rangle_{\rm el} = 2\langle\mathcal{O}\rangle_m - \langle\mathcal{O}\rangle_v, \tag{10}$$

or

$$\langle\mathcal{O}\rangle_{\rm eq} = \frac{\langle\mathcal{O}\rangle_m^2}{\langle\mathcal{O}\rangle_v}, \tag{11}$$

$\langle\mathcal{O}\rangle_v$ being a variational Monte Carlo estimation. Both $\langle\mathcal{O}\rangle_{\rm el}$ and $\langle\mathcal{O}\rangle_{\rm eq}$ are accurate to first order in $\delta\Psi$, with $\Psi_T=\Phi_0+\delta\Psi$, but in general it is not enough to completely eliminate the influence of Ψ_T in $\langle\mathcal{O}\rangle$. In order to go beyond this approximation, we have used for the expectation values of coordinate operators the pure estimators following the methodology of Ref. 13 based on the future-walking strategy.[22] As proved in pure ^{4}He,[13] the pure estimator removes all the dependence on Ψ_T providing results as exact as the ones for the total energy.

Derivative operators as the kinetic energy cannot be evaluated with the pure estimator, and the extrapolation methods generate more unreliable results than in the case of $\mathcal{O}(\mathbf{R})$. In a pure phase it is not a severe problem because the kinetic energy can be calculated through the difference $E/N-V/N, V/N$ being the pure estimation of the potential energy. That it is not obviously possible in the impurity system because the total energy includes the kinetic energy of the medium and the one of the ^{3}He impurity. To overcome this difficulty and go to an unbiased estimation of the ^{3}He kinetic energy one can invoke the Hellmann-Feynman theorem.[23] It states that

$$\langle T_I\rangle = D_I\frac{\partial E}{\partial D_I}, \tag{12}$$

E being the exact ground-state energy. We have then evaluated T_I discretizing the derivative $\partial E/\partial D_I$ and computing the difference in the total energy (with $\Delta D_I/D_I=0.1-10\%$) by means of the generalized reweighting method.

III. RESULTS

The microscopic properties of a ^{3}He atom immersed in bulk ^{4}He have been investigated putting it in a simulation box with $N-1$ ^{4}He atoms in such a way that the volume is $\Omega=N/\rho$, with ρ the input density. In all the simulations $N=108$ particles have been used and the time step and population bias have been analyzed in order to remove any systematic error. We have also verified that for $N\gtrsim 100$ the finite-system size introduces an error which is smaller than the statistical noise, indicating that the influence of the replicas of the ^{3}He impurity implied by the use of periodic boundary conditions is negligible. The interatomic interaction, which does not distinguish between the two isotopes, is the HFD-B(HE) Aziz potential[24] which has proved its high accuracy in a DMC calculation of the equation of state of superfluid ^{4}He at zero temperature.[19,20] Concerning the trial wave function (5), the two-body factor proposed in Ref. 25 with the parameters optimized for pure ^{4}He (Ref. 19) has been considered.

We present the results of our calculations starting with a microscopic analysis of the local environment of the ^{3}He impurity in the medium. This information is mainly contained in the crossed two-body radial distribution function $g^{(4,I)}(r)$. In Fig. 1, mixed (short-dashed line) and pure (solid line) estimations of $g^{(4,I)}(r)$ at densities 0.365, 0.401, and 0.424 σ^{-3} ($\sigma=2.556$ Å) are reported. In all the three densities the pure or exact results appear shifted to the right with respect to the mixed estimations pointing to a larger hole that is absolutely absent in the trial wave function. On the other hand, the height of the main peak in the pure $g^{(4,I)}(r)$ is slightly reduced at positive pressures and remains

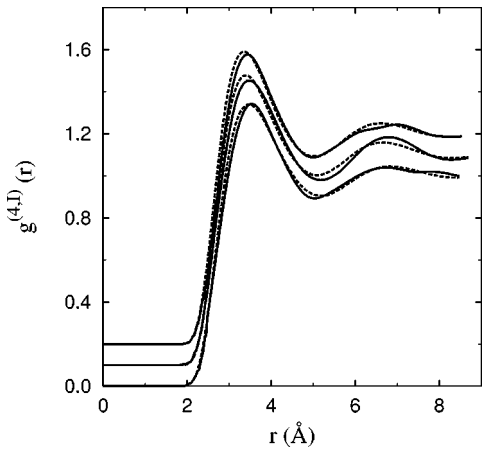

FIG. 1. Mixed (dashed line) and pure (solid line) estimations of $g^{(4,I)}(r)$ at densities 0.365 σ^{-3}, 0.401 σ^{-3}, and 0.424 σ^{-3}, from bottom to top. A vertical shift has been introduced at 0.401 σ^{-3} and 0.424 σ^{-3} to better visualize their differences.

unchanged at the equilibrium density. In Fig. 2, the evolution of $g^{(4,I)}(r)$ with density is compared with the one shown by the pure ^{4}He distribution function $g^{(4,4)}(r)$. Both functions show an increase of the localization when the density increases as well as a shift of the main peak to shorter interparticle distances. At a given density, the height of the main peak of $g^{(4,I)}(r)$ is smaller than the one of $g^{(4,4)}(r)$ and, what is more relevant, it appears localized to the right of the main peak of $g^{(4,4)}(r)$ pointing manifestly to the existence of an excluded-volume region due to the smaller mass of the ^{3}He atom. The size of the excluded volume decreases when the density increases as one qualitatively can see comparing $g^{(4,4)}(r)$ and $g^{(4,I)}(r)$ at equilibrium and at the highest density plotted in Fig. 2.

Additional information on the local environment of the impurity is contained in the crossed static structure factor $S^{(4,I)}(k)$,

$$S^{(4,I)}(k)=\left\langle \Phi_0 \left| e^{i\mathbf{k}\cdot\mathbf{r}_I} \sum_{i=1}^{N-1} e^{-i\mathbf{k}\cdot\mathbf{r}_i} \right| \Phi_0 \right\rangle, \tag{13}$$

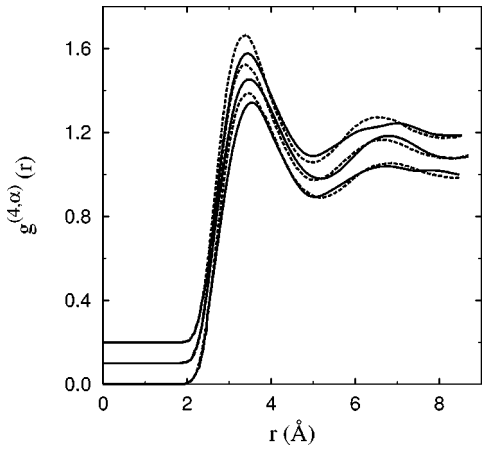

FIG. 2. Pure liquid ^{4}He (dashed line) and impurity-medium (solid line) two-body radial distribution functions at densities 0.365 σ^{-3}, 0.401 σ^{-3}, and 0.424 σ^{-3}, from bottom to top. A vertical shift has been introduced at 0.401 σ^{-3} and 0.424 σ^{-3} to better visualize their differences.

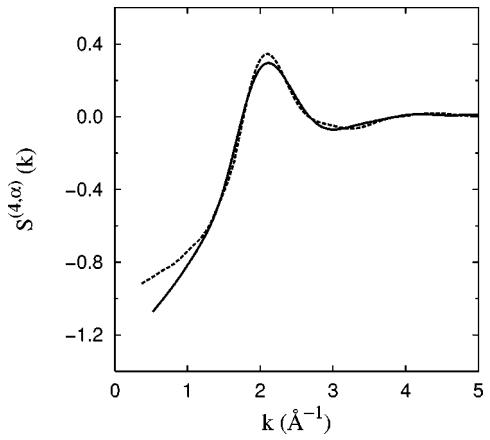

FIG. 3. Pure liquid ^{4}He (dashed line) and impurity-medium (solid line) static structure factor at the ^{4}He equilibrium density $\rho_0=0.365$ σ^{-3}. We have plotted $S^{(4,4)}(k)-1$ for a better comparison.

which corresponds to the Fourier transform of $g^{(4,I)}(r)$

$$S^{(4,I)}(k)=\rho\int d\mathbf{r}\, e^{i\mathbf{k}\cdot\mathbf{r}}[g^{(4,I)}(r)-1], \tag{14}$$

ρ being the density of pure ^{4}He. From the above definition it is easy to check that the value of $S^{(4,I)}(k)$ at the origin is[7,8]

$$S^{(4,I)}(0+)=-(1+\alpha) \tag{15}$$

with $\alpha=v/v_4$ being the quotient between the molar volume of the impurity system (v) and that of pure ^{4}He (v_4). In Fig. 3, $S^{(4,I)}(k)$ is plotted in comparison with $S^{(4,4)}(k)-1$ at the ^{4}He equilibrium density, $S^{(4,4)}(k)$ being the pure ^{4}He static structure factor

$$S^{(4,4)}(k)=1+\rho\int d\mathbf{r}\, e^{i\mathbf{k}\cdot\mathbf{r}}[g^{(4,4)}(r)-1]. \tag{16}$$

The function $S^{(4,I)}(k)$ shown in the figure has been obtained Fourier transforming $g^{(4,I)}(r)$ for values $k>1$ Å^{-1} and by a direct calculation of Eq. (13) for $k\leqslant 1$ Å^{-1}. The main peak of $S^{(4,I)}(k)$ appears slightly depressed with respect to the one of $S^{(4,4)}(k)-1$ reflecting the same feature observed in the comparison of the radial distribution functions. Nevertheless, the largest differences between the two static structure functions are at low k values ($k\leqslant 1$ Å^{-1}). In spite of the impossibility of calculating $S^{(4,\alpha)}(k)$ below a certain $k_{\min}$, imposed by the use of a finite-size simulation box and periodic boundary conditions, if a linear extrapolation to $k=0$ is carried out one obtains $S^{(4,4)}(0)-1\simeq -1$ and $S^{(4,I)}(0)\simeq -1.3$. If the latter is compared with Eq. (15), it results $\alpha=0.3$ to be compared with the experimental value $\alpha^{\text{expt}}=0.284$.[1] The volume-excess parameter α decreases with pressure but this feature may be hardly observed in the limiting behavior of $S^{(4,I)}(k)$ at different densities (Fig. 4).

One of the most relevant magnitudes in the study of the impurity system is the binding energy of the ^{3}He atom in the medium or, otherwise, the chemical potential of the impurity μ_I. In Table I, we report DMC results of the pure ^{4}He chemical potential μ_4 and μ_I at three densities which correspond to the pressures also contained in the table. The results

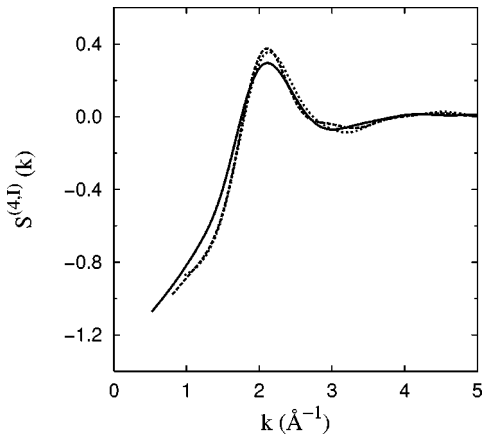

FIG. 4. Impurity-medium static structure factor at densities 0.365 σ^{-3} (solid line), 0.401 σ^{-3} (dashed line), and 0.424 σ^{-3} (dotted line).

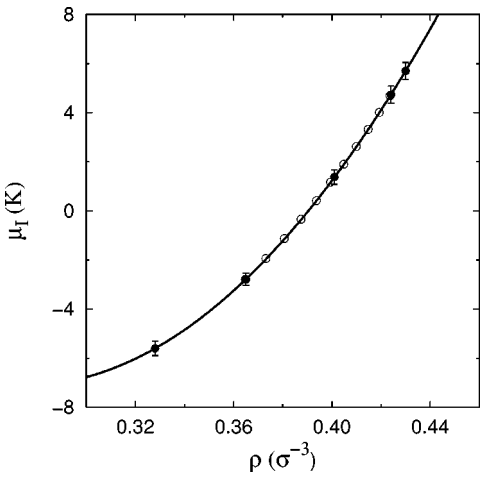

FIG. 5. Chemical potential of the ^{3}He impurity as a function of the density (full circles). The solid line is a polynomial fit to the DMC results. The open circles are experimental data from Ref. 1.

for the pressure and μ_4 reproduce the experimental data with high accuracy as pointed out in Refs. 19,20. Also, in the present case, one gets a good agreement between the calculated μ_I and the experimental data,[1] the statistical uncertainties in the values of μ_I being less than 10%. A more exhaustive comparison between theoretical and experimental values for μ_I is displayed in Fig. 5. In the figure, two additional results are plotted: one at a pressure higher than 20 atm, and another located at a density smaller than the equilibrium one (ρ_0) which corresponds to a negative pressure of -6 atm. The solid line is a polynomial fit to the DMC results and has to be compared with the available experimental data of Ref. 1, also reported in the figure. As one can see, the agreement between theory and experiment is excellent and a minimum in $\mu_I(\rho)$ is not observed in this region. In fact, if a minimum exists it is located at lower densities, even below the spinodal density of ^{4}He ($\rho_s=0.264\ \sigma^{-3}$).[20] It is worth noticing that ^{3}He energetically prefers to remain in the surface of liquid ^{4}He forming an Andreev state rather than penetrate in the bulk.[26,27] We have verified[28] that if the ^{3}He impurity is replaced by a H_2 molecule there is a minimum of μ_I at a density below ρ_0 that nearly coincides with the local density of the preferred location of H_2 in ^{4}He clusters obtained in a DMC calculation of Barnett and Whaley.[29]

In ACA the chemical potential of the impurity is given by[9,30]

$$\mu_I^{\mathrm{ACA}}=\mu_4+\left(\frac{m_4}{m_I}-1\right)T_4, \tag{17}$$

i.e., it can be calculated from the knowledge of properties of the pure liquid. This approximation provides upper bounds (see Table I) which, using DMC values for μ_4 and T_4, come close to the DMC and experimental values.

The volume-excess parameter α may be obtained from the knowledge of $\mu_I(\rho)$, or equivalently $\mu_I(P)$, through the thermodynamic relation

$$\alpha=\rho\frac{\partial\mu_I}{\partial P}-1. \tag{18}$$

The values for α so obtained are reported in Table I in comparison with the experimental data of Ref. 1. The agreement between α and α^{expt} is very good at zero and intermediate pressures and even at high pressure where the error bar is somewhat larger.

Microscopic quantities which are also significant in the present study are the kinetic energy of the ^{3}He atom and the mean potential energy ^{3}He-^{4}He (V_I). In Table II, results for the kinetic and potential energies for the two helium isotopes are reported at several densities. All of them correspond to pure estimations. In both systems, pure liquid ^{4}He and liquid ^{4}He with one ^{3}He impurity, the potential energies may be obtained using the same method that has been used for the radial distribution functions because they are coordinate operators. The pure ^{4}He kinetic energy simply results from the difference $E/N-V/N$ but that is not the case for T_I in the impurity system due to the coexistence of the two isotopes. Therefore, the kinetic energy of the impurity has been calculated using the Hellmann-Feynman theorem as commented in Sec. II. The ACA estimation of the partial energies of the impurity is $T_I^{\mathrm{ACA}}=m_4/m_I\ T_4$ and $V_I^{\mathrm{ACA}}=V_4$, the values of T_I^{ACA} being explicitly given in Table II to be compared with the exact results. In going from T_4 to T_I one can see that the

TABLE I. Chemical potential of pure liquid ^{4}He (μ_4), chemical potential of the ^{3}He impurity (μ_I), and excess-volume parameter α at several densities. The experimental data are from Ref. 1.

ρ (σ^{-3})	P(atm)	μ_4 (K)	μ_I^{ACA} (K)	μ_I (K)	μ_I^{expt} (K)	α	α^{expt}
0.365	0.	−7.27(1)	−2.58	−2.79(25)	−2.785	0.284(10)	0.284
0.401	10.67	−3.89(1)	1.59	1.38(30)	1.42	0.200(10)	0.199
0.424	20.42	−0.97(2)	5.10	4.73(35)	4.83	0.176(20)	0.165

TABLE II. Kinetic and potential energies of the pure liquid ^{4}He and of the ^{3}He impurity immersed in bulk ^{4}He. All the energies are in K.

ρ (σ^{-3})	T_4	V_4	$T_I^{\rm ACA}$	T_I	V_I
0.328	11.99(8)	−19.14(6)	15.91(8)	17.0(6)	−18.2(5)
0.365	14.32(5)	−21.59(5)	19.00(7)	18.4(5)	−21.1(5)
0.401	16.73(9)	−23.88(9)	22.20(12)	20.5(5)	−22.6(5)
0.424	18.57(8)	−25.45(8)	24.64(11)	23.4(8)	−24.7(5)

largest change is due to the difference in the mass of the two isotopes, the only effect contained in $T_I^{\rm ACA}$, and the correction due to different correlations, i.e., $T_I^{\rm ACA}-T_I$, is in all cases less than 10%. This small correction is also observed by comparing V_4 and V_I. In the range of densities here analyzed, it is observed that V_I is always smaller than V_4 (in absolute value) whereas the difference $T_I^{\rm ACA}-T_I$ is not monotonous: at $P\geqslant 0, T_I^{\rm ACA}>T_I$ but $T_I^{\rm ACA}<T_I$ at a density 0.328 σ^{-3} ($P=-6$ atm). This striking behavior can be better understood looking at the differences between $g^{(4,I)}_{\rm ACA}(r)=g^{(4,4)}(r)$ and $g^{(4,I)}(r)$ at each density. In the region of positive and zero pressures the main peak of $g^{(4,I)}(r)$ is ever shifted to the right with respect to the one of $g^{(4,4)}(r)$ and with a smaller localization (Fig. 2). The environment of the impurity may then be made *equivalent* to a pure ^{4}He liquid at a reduced density. The reduced density ρ_r of the *equivalent* system at positive pressure can be obtained by looking for the density of pure ^{4}He at which V_I and $g^{(4,I)}(r)$ do correspond. If the density ρ_r is then used to estimate the kinetic energy of the impurity, $T_I(\rho_r)=m_4/m_I\ T_4(\rho_r)$, the results for T_I are the same than the ones reported in Table II. This supplies an additional test to our pure computation of T_I using the Hellmann-Feynman theorem. In the case of the equilibrium density ($\rho_0=0.365\ \sigma^{-3}$) $\rho_r=0.358\ \sigma^{-3}$. At ρ_r, we have performed an explicit calculation of ^{4}He and have verified that $g^{(4,4)}(r)$ is very much the same that $g^{(4,I)}(r)$ at ρ_0. On the other hand, at the lowest density reported in Table II ($\rho=0.328\ \sigma^{-3}$, $P=-6$ atm) the *equivalent* system does not exist because the shift of the main peak of $g^{(4,I)}(r)$ with respect to the one of $g^{(4,4)}(r)$ disappears and only a small delocalization remains.

There is only a previous *ab initio* calculation of T_I at the ^{4}He equilibrium density using PIMC and extrapolating to zero temperature.[12] Our present result for T_I, which is more accurate than our preliminary result of Ref. 31, is appreciably larger than the value reported in Ref. 12, $T_I=17.1(1)$ K. As a kind of closure test of our results we have calculated the mass dependence of T_I in order to estimate the chemical potential of the ^{3}He impurity through the relation

$$\mu_I=\mu_4+\int_{m_I}^{m_4} dm\,\frac{T_I(m)}{m}. \tag{19}$$

In Fig. 6, results for T_I using different masses for the impurity are displayed in comparison with the ACA prediction (dashed line). For simplicity, the kinetic energies T_I correspond in this case to mixed estimations, since at ρ_0 and for

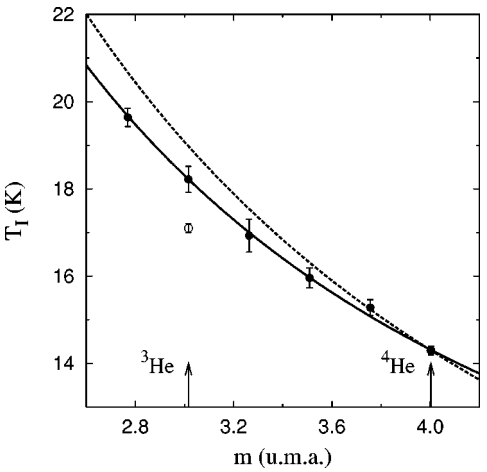

FIG. 6. Kinetic energy of the impurity as a function of its mass (full circles and solid line). The dashed line corresponds to the ACA prediction. The open circle is the PIMC result from Ref. 12.

the aforementioned trial wave function the mixed and pure results coincide for both $m_I=m_4$ and $m_I=m_3$. The PIMC result for $m_I=m_3$ is also shown as an open circle. In the ACA case, if T_I in Eq. (19) is replaced by $T_I^{\rm ACA}$ one recovers the ACA expression for μ_I Eq. (17) and the corresponding result reported in Table I, $\mu_I^{\rm ACA}=-2.58$ K. The solid line in Fig. 6 corresponds to a fit $T_I(m)=am+b/m$, and when integrated in Eq. (19) one obtains $\mu_I=-2.70(10)$ K which is consistent with both the experimental value and our direct estimation contained in Table I. As a supplementary result, it is predicted a linear departure from the ACA prediction with the impurity mass as is clearly manifested in Fig. 7, where the function $T_I^{\rm ACA}(m)-T_I(m)$ is shown. Finally, it is worth mentioning that our results confirm and even enlarge the discrepancies between deep-inelastic neutron-scattering determinations of the ^{3}He kinetic energy in liquid ^{3}He-^{4}He mixtures[3,4] ($T_3=11\pm 3$ K at $P=0$ and $x=N_3/N=0.10$) and all the theoretical predictions.[5,6,12] One of the reasons that may explain this disturbing difference is the importance of the high-energy tails in the dynamic structure function which largely influence the second energy-weighted sum rule from which the kinetic energy is extracted.

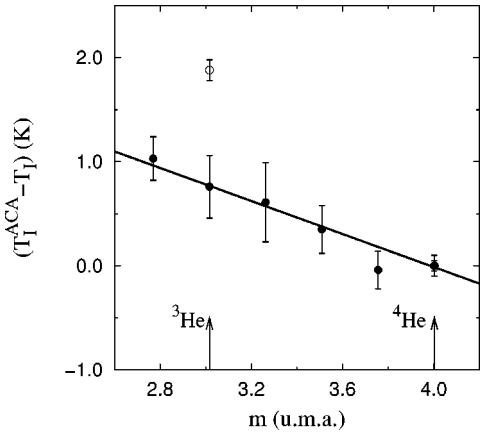

FIG. 7. Difference between the ACA prediction and the real value for the kinetic energy of the impurity as a function of its mass (full circles and solid line). The open circle is the PIMC result from Ref. 12.

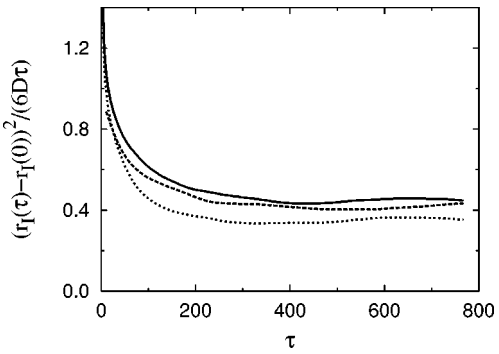

FIG. 8. The inverse of the impurity effective mass from the long-time behavior of its diffusion coefficient. The solid, dashed, and dotted lines correspond to densities 0.365 σ^{-3}, 0.401 σ^{-3}, and 0.424 σ^{-3}, respectively.

We close this section with the results obtained for the impurity effective mass $m_I^\star$, which has been recently measured with great accuracy in ^{3}He-^{4}He mixtures[14,15] and also microscopically analyzed using correlated basis function (CBF) theory.[10] The ^{3}He effective mass plays a relevant role in the study of ^{3}He-^{4}He mixtures characterizing the ^{3}He excitations at low momenta. In a DMC calculation, the impurity effective mass can be obtained from the diffusion coefficient of the impurity in imaginary time[12]

$$\frac{m_I}{m_I^\star}=\lim_{\tau\to\infty}\frac{|\mathbf{r}_I(\tau)-\mathbf{r}_I(0)|^2}{6D_I\tau}, \tag{20}$$

with $D_I=\hbar^2/(2m_I)$ the free-diffusion constant of the impurity. In Fig. 8, extrapolated estimations of $m_I/m_I^\star$ are reported at densities 0.365, 0.401, and 0.424 σ^{-3}. The impurity effective mass is extracted from a linear fit to the flat asymptotic regime of that function (20) which, as the figure shows, is acquired at relatively short diffusion times. The results so obtained are reported in Table III in comparison with the experimental determinations from Refs. 14,15 and the recent CBF calculation of Krotscheck *et al.*[10] Obviously, the experimental values are not direct measures but extrapolations to zero ^{3}He concentration (x) of determinations in ^{3}He-^{4}He mixtures. As pointed out by Krotscheck *et al.*[10] a linear extrapolation, primarily used in the experimental works, is not satisfactory because the Fermi-liquid contributions are the most relevant in the ^{3}He-concentration dependence of $m_I^\star$ and these terms introduce fractional powers of x in the analytical model for $m_I^\star(x)$. The experimental values reported in Table III have been obtained using this more accurate extrapolation. Within the statistical errors of the DMC results, an overall agreement between our calculation and experiments is attained, with somehow a significant difference at the highest density due in part to the use of the extrapolated estimation (10). On the other hand, the CBF results of Ref. 10 come close to the DMC and experimental results but seem to be slightly smaller at the densities here reported. Another CBF calculation, due to Fabrocini *et al.*,[32] reported several years ago a result of $m_I^\star=2.2$ at the equilibrium density in better agreement with the present DMC results.

TABLE III. ^{3}He impurity effective mass at several densities. The CBF results are from Ref. 10.

ρ (σ^{-3})	$m_I^\star$	$m_I^{\star\,\mathrm{expt}}$ (Ref. 14)	$m_I^{\star\,\mathrm{expt}}$ (Ref. 15)	$m_I^{\star\,\mathrm{CBF}}$
0.365	2.20(5)	2.18	2.15	2.09
0.401	2.36(8)	2.44	2.39	2.34
0.424	2.72(10)	2.64	2.62	2.55

IV. SUMMARY AND CONCLUSIONS

We have analyzed in this paper the most important magnitudes which characterize the static properties of a single ^{3}He atom embedded in bulk superfluid ^{4}He. The difficulties of an efficient calculation of the binding energy of the impurity in the medium, one of the main objectives of the present work, had prevented in the past the application of *ab initio* Monte Carlo methods to this problem. In order to overcome these difficulties, it has been proved that the use of reweighting techniques can be readily extended to diffusion Monte Carlo algorithms. This generalized reweighting method has provided reliable results for μ_I which are in excellent agreement with experimental data.

The local environment of the ^{3}He atom has been explored through the calculation of the crossed radial distribution and static structure functions for a wide range of densities. The use of pure estimators for these quantities removes the uncontrolled bias, remanent in the approximate extrapolation methods, and shows clear evidence of an excluded volume region surrounding the ^{3}He impurity. The low k behavior of $S^{(4,I)}(k)$ also points to the expected value related to the volume-excess parameter α, but a precise value for α cannot be estimated due to the absence of data for $k\leqslant k_{\min}=2\pi/L$, with L the side of the simulation box. Nevertheless, an independent and more precise estimation of α, through the pressure dependence of the chemical potential of the impurity, produces results which compare favorably with experimental data.

Special attention has been devoted to an accurate estimation of the partial energies, potential and kinetic, of the impurity. The usual forward walking methodology does not apply for derivative operators, and for this reason, we have used the Hellmann-Feynman theorem combined with the generalized reweighting method to calculate the ^{3}He kinetic energy. The results for T_I obtained with this method show smaller differences with the ACA values than a previous PIMC estimate,[12] with a difference $T_I^{\mathrm{ACA}}-T_I$ which increases linearly with the mass of the isotopic impurity. Our results confirm the gap between all the theoretical results for T_I and the much smaller ^{3}He kinetic energies derived from the neutron-scattering data of Refs. 3,4.

A final concern of the present work is the calculation of the ^{3}He effective mass through its diffusion coefficient in imaginary time. The results obtained show a good agreement with recent experimental data that slightly worsens at high pressure due probably to uncertainties in the MC extrapolation method used in the estimation of $m_I^\star$. A natural extension to the present work would be the calculation of the

excitation energy of the ^{3}He impurity in liquid ^{4}He, which in the limit $q \to 0$ is given by $\hbar^2 q^2/2m_I^\star$, and therefore will provide another method to estimate the impurity effective mass. In such a calculation, one can use DMC combined with the fixed-node and released-node methods, that we have already employed in the study of the phonon-roton spectrum in superfluid ^{4}He.[33] Work in this direction is in progress.

ACKNOWLEDGMENTS

J.B. is grateful for useful discussions with Artur Polls who initiated him into the physics of impurities in superfluid ^{4}He. This work has been supported in part by DGICYT (Spain) Grant No. PB96-0170-C03-02 and No. TIC95-0429. We also acknowledge the supercomputer facilities provided by the CEPBA.

[1] C. Ebner and D. O. Edwards, Phys. Rep., Phys. Lett. **2C**, 77 (1971).

[2] D. O. Edwards and M. S. Petersen, J. Low Temp. Phys. **87**, 473 (1992).

[3] Y. Wang and P. E. Sokol, Phys. Rev. Lett. **72**, 1040 (1994).

[4] R. T. Azuah, W. G. Stirling, J. Mayers, I. F. Bailey, and P. E. Sokol, Phys. Rev. B **51**, 6780 (1995).

[5] S. Moroni and M. Boninsegni, Europhys. Lett. **40**, 287 (1997).

[6] J. Boronat, A. Polls, and A. Fabrocini, Phys. Rev. B **56**, 11 854 (1997).

[7] M. Saarela and E. Krotscheck, J. Low Temp. Phys. **90**, 415 (1993).

[8] A. Fabrocini and A. Polls, Phys. Rev. B **30**, 1200 (1984).

[9] J. Boronat, A. Fabrocini, and A. Polls, J. Low Temp. Phys. **74**, 347 (1989).

[10] E. Krotscheck, M. Saarela, K. Schörkhuber, and R. Zillich, Phys. Rev. Lett. **80**, 4709 (1998).

[11] K. E. Kürten and M. L. Ristig, Nuovo Cimento D **7**, 251 (1986).

[12] M. Boninsegni and D. M. Ceperley, Phys. Rev. Lett. **74**, 2288 (1995).

[13] J. Casulleras and J. Boronat, Phys. Rev. B **52**, 3654 (1995).

[14] S. Yorozu, H. Fukuyama, and H. Ishimoto, Phys. Rev. B **48**, 9660 (1993).

[15] R. Simmons and R. M. Mueller, Czech. J. Phys. **46**, 201 (1996).

[16] J. B. Anderson, J. Chem. Phys. **63**, 1499 (1975).

[17] P. J. Reynolds, D. M. Ceperley, B. J. Alder, and W. A. Lester, Jr., J. Chem. Phys. **77**, 5593 (1982).

[18] B. J. Hammond, W. A. Lester, Jr., and P. J. Reynolds, *Monte Carlo Methods in Ab Initio Quantum Chemistry* (World Scientific, Singapore, 1994).

[19] J. Boronat and J. Casulleras, Phys. Rev. B **49**, 8920 (1994).

[20] J. Boronat, J. Casulleras, and J. Navarro, Phys. Rev. B **50**, 3427 (1994).

[21] D. M. Ceperley and M. H. Kalos, in *Monte Carlo Methods in Statistical Physics*, edited by K. Binder (Springer-Verlag, Berlin, 1979).

[22] K. S. Liu, M. H. Kalos, and G. V. Chester, Phys. Rev. A **10**, 303 (1974).

[23] The origin of the Hellmann-Feynman theorem is discussed by J. I. Musher, Am. J. Phys. **34**, 267 (1966).

[24] R. A. Aziz, F. R. W. McCourt, and C. C. K. Wong, Mol. Phys. **61**, 1487 (1987).

[25] L. Reatto, Nucl. Phys. A **328**, 253 (1979).

[26] A. F. Andreev, Sov. Phys. JETP **23**, 939 (1966).

[27] D. O. Edwards and W. F. Saam, in *Progress in Low Temperature Physics*, edited by D. F. Brewer (North-Holland, Amsterdam, 1978), Vol. VII A, p. 283.

[28] J. M. Marín, J. Boronat, and J. Casulleras (unpublished).

[29] R. N. Barnett and K. B. Whaley, J. Chem. Phys. **96**, 2953 (1992).

[30] G. Baym, Phys. Rev. Lett. **17**, 952 (1966).

[31] J. Boronat, J. Casulleras, and A. Polls, Czech. J. Phys. **46**, 271 (1996).

[32] A. Fabrocini, S. Fantoni, S. Rosati, and A. Polls, Phys. Rev. B **33**, 6057 (1986).

[33] J. Boronat and J. Casulleras, Europhys. Lett. **38**, 291 (1997).